

Articulatory Encodec: Vocal Tract Kinematics as a Codec for Speech

Cheol Jun Cho, Peter Wu, Tejas S. Prabhune, Dhruv Agarwal, and Gopala K. Anumanchipalli

Abstract—Vocal tract articulation is a natural, grounded control space of speech production. The spatiotemporal coordination of articulators combined with the vocal source shapes intelligible speech sounds to enable effective spoken communication. Based on this physiological grounding of speech, we propose a new framework of neural encoding-decoding of speech – *articulatory encodec*. The articulatory encodec comprises an articulatory analysis model that infers articulatory features from speech audio, and an articulatory synthesis model that synthesizes speech audio from articulatory features. The articulatory features are kinematic traces of vocal tract articulators and source features, which are intuitively interpretable and controllable, being the actual physical interface of speech production. An additional speaker identity encoder is jointly trained with the articulatory synthesizer to inform the voice texture of individual speakers. By training on large-scale speech data, we achieve a fully intelligible, high-quality articulatory synthesizer that generalizes to unseen speakers. Furthermore, the speaker embedding is effectively disentangled from articulations, which enables accent-perserving zero-shot voice conversion. To the best of our knowledge, this is the first demonstration of universal, high-performance articulatory inference and synthesis, suggesting the proposed framework as a powerful coding system of speech.

Index Terms—neural codec, speech coding, speech synthesis, articulatory synthesis, speech inversion, acoustics-to-articulatory inversion, electromagnetic articulography.

I. INTRODUCTION

Humans naturally produce intelligible speech by controlling articulators on the vocal tract. Such vocal tract articulation has long been claimed to be the physiological ground of speech production in various aspects. The source-filter theory of speech describes articulation as shaping the vocal cavity to implement filters that are applied to glottal flow to shape speech sounds [1], [2]. Articulatory phonetics and phonology have explained the basis of speech in terms of the coordination of articulators, identifying some canonical articulators that can determine the phonetic properties [3], [4], [5]. From deep down in the brain, the speech sensorimotor cortex has been proven to represent continuous, real-time vocal tract articulation while naturally speaking, suggesting the vocal tract articulation as a cognitive basis of speech production [6], [7], [8].

Furthermore, the recent findings by Cho et al. [9], [10] suggest that articulatory inversion naturally emerges from self-supervised learning (SSL) of speech. When probed on articulatory kinematics measured by electromagnetic articulography

All authors are with the Department of Electrical Engineering and Computer Sciences at University of California, Berkeley (e-mail: cheoljun@berkeley.edu; peterw1@berkeley.edu; prabhune@berkeley.edu; dhruvagarwal@berkeley.edu; gopala@berkeley.edu).

Corresponding author: Cheol Jun Cho; Gopala K. Anumanchipalli

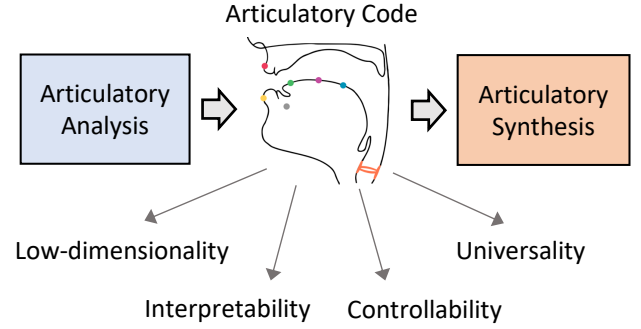


Fig. 1. Articulatory encodec framework.

(EMA), the features representation of the recent speech SSL models (e.g., HuBERT [11]) is highly correlated with EMA, where high-fidelity articulation can be reconstructed by a simple linear mapping from speech SSL features [9]. This suggests that the articulatory inference is a natural solution of SSL of speech for abstracting the speech information. This emergent property is further shown to be universal to any speakers, dialects, and even languages [10]. Together, these suggest that the biophysical, articulatory representation of speech is a shared coding principle in both biological and artificial intelligence of speech.

However, despite the ubiquity of articulatory coding in speech science, an effective and scalable articulatory coding system for speech has not yet been demonstrated, which requires a generalizable articulatory synthesis model that synthesizes speech back from the articulatory inputs, along with a robust encoding model for articulatory features. Previous studies have demonstrated that intelligible speech can be synthesized from articulatory features [12], [13], [14], [15], [16]. Combined with acoustics-to-articulatory inversion (AAI), resynthesis frameworks have shown the potential of articulatory features as viable intermediate for speech coding systems [17], [16]. However, the previous methods are limited to a fixed set of speakers and the qualities are still far behind the commercial speech synthesis models. This absence of a universal, generalizable framework has significantly limited the utility of articulatory-based speech coding as a practically usable system.

Here, we first demonstrate a high-performance, universal articulatory encoder and decoder that can scale and generalize across an indefinite number of speakers. We leverage the universal articulatory inference by speech SSL [10] to build a generalizable articulatory encoder that transforms speech into a template articulatory space. The template articulatory space

is agnostic to individual anatomical differences which are compensated by a separate speaker identity encoder. By training a vocoder with a large-scale dataset, we achieve a universal articulatory vocoder that can generate fully intelligible, high-quality speech from any speaker’s articulation. Furthermore, the speaker embedding learned by the speaker identity encoder enables a zero-shot, dialect-preserving voice conversion. By closing the loop of articulatory encoding and decoding, we propose a novel, speech science guided encoding-decoding (encodec) framework of speech – *articulatory encodec*.¹ The articulatory encodec shows a minimal loss of intelligibility and quality compared to the original speech audio.

Compared to existing neural coding of speech [18], [19], [20], [21], [22], representing speech as articulatory features has following benefits:

- **Low-dimensionality:** The articulatory features have only 14 channels with 50 Hz sampling rate. This is significantly lower than the previous acoustic features or neural embedding of speech.
- **Interpretability:** Each channel corresponds to the actual physical articulator on the vocal tract, which can be intuitively interpretable by visualization on the vocal tract.
- **Controllability:** The articulatory features can be naturally controlled by the same principle as speech production.
- **Universality:** The articulatory encoding is universal across speakers despite and disentangled from individual anatomical variance.

With these unique benefits, empirical evidence and demonstration show the promising potential of the proposed articulatory encodec as a valid, novel coding framework of speech.²

II. RELATED WORK

A. Electromagnetic Articulography

Electromagnetic articulography (EMA) measures time-varying displacements of vocal tract articulators synchronously while speaking. Typically, sensors are placed on the upper lip (UL), lower lip (LL), lower incisor (LI), tongue tip (TT), tongue blade (TB), and tongue dorsum (TD) (Fig. 2) [23]. A combination of displacements of these articulators on the midsagittal plane configures a place of articulation, which shapes phonetic content by combining with source information, or manner of articulation. As the traces are continuously collected in real-time, the EMA data naturally reflect phoneme contextualization, or coarticulation, and individual tendencies in pronunciations (dialects and accents). Given these properties, EMA has been widely accepted for studying articulatory bases of speech, providing biophysical evidence for many linguistic or cognitive theories of speech production [4], [23], [6]. However, EMA has been significantly limited to scale due to the complicated nature and high cost of the collection procedure.

B. Acoustics-to-Articulation Inversion

To replace the complicated data collection procedure, acoustic-to-articulatory inversion (AAI) models have been actively developed to predict EMA directly from speech audio [24], [25], [26], [6], [7], [17], [27], [28], [16]. However, the individual variance in vocal tract anatomy across speakers induces inconsistent placements of sensors, which has posed a significant barrier to developing a model that can apply to unseen speakers [29], [17], [27], [28]. Despite such variability, a canonical basis of articulation is suggested to exist, which is agnostic to individual vocal tract anatomy [10]. In fact, Cho et al. [10] demonstrated that a linear affine transformation can geometrically align one speaker’s articulatory system to another’s. This suggests that individual articulatory spaces are lying on the same linear space so that an articulatory space of any speaker can be a hypothetical universal template space of articulation. We empirically prove this statement by leveraging a single-speaker AAI model as a universal articulatory encoder for our codec framework.

C. Articulatory Synthesis

Articulatory synthesis aims to generate speech audio from articulatory features. A century of efforts have been made to build articulatory synthesizers for basic research of speech [30], [31], [32], [33], [34], [35], [36], [37], [38]. Several methods have been proposed for improving intelligibility and quality, demonstrating broader use cases including text-to-speech (TTS) [13], prosody manipulation [39], [40], and speech brain-computer interfaces (BCIs) [7]. Some of these works utilized deep learning models to map articulatory features to acoustic features, which are then converted to audio using pretrained acoustic synthesizers [41], [7], [15]. A recent study shows that a GAN-based generative model can directly synthesize speech waveform from articulatory features with high intelligibility [14]. However, to our knowledge, none of the existing approaches has achieved industrial-level performance, which requires high intelligibility, quality, and generalizability across unseen speakers.

D. Neural Codec of Speech

Many deep learning methods have been proposed to learn data-driven representations of speech. Various autoencoder methods have been suggested to jointly train encoders that compress audio into low-bitrate discrete units [42], [20], [21] or decompose speech into different factors [19], [43], [22], and decoders that reconstruct speech from encoded features with minimal loss of information. Also, pretrained speech SSL models have been utilized to extract rich linguistic content of speech, and synthesizers are trained to restore speech audio from those features [18], [44], [19], [45], [46], [47]. These SSL-based methods often utilize separate source modeling (e.g., pitch) and speaker encoding, since SSL model encoders tend to marginalize out acoustic and speaker information [48], [49]. We categorize all these kinds of closed-loop frameworks utilizing neural networks for both encoding and decoding as *neural codecs*. Though the existing methods achieve high

¹We will open-source the code and model checkpoints upon publication.

²Audio samples are available at <https://articulatoryencodec.github.io>.

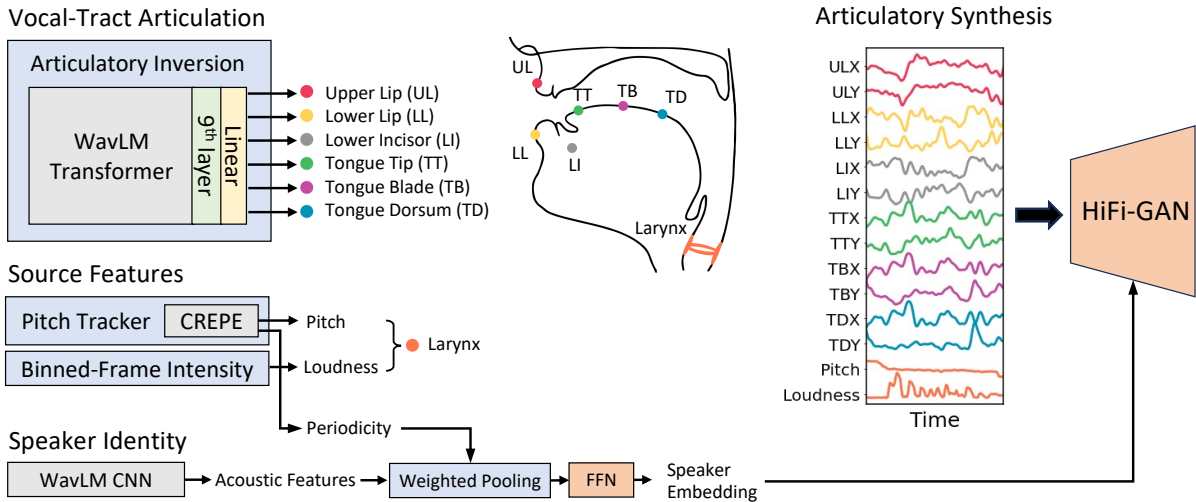


Fig. 2. Pipeline of articulatory analysis and vocoder. The articulatory analysis is composed of vocal-tract articulation, source features, and speaker embedding, which are then fed to the synthesizer (HiFi-GAN) in the synthesis pipeline. The modules colored with orange are updated while training the vocoder and other modules are fixed.

fidelity in representing speech audio, they significantly lack interpretability and controllability.

III. METHODS

To bridge this interpretability and controllability gap, we propose neural articulatory inversion and synthesis as a new type of neural codec that can provide an interpretable and controllable coding of speech.

A. Articulatory Analysis

The articulatory encoding is extracted by articulatory analysis of 3 different aspects of speech: vocal-tract articulation, source features, and speaker identity (Fig. 2).

1) *Vocal-tract articulation*: Based on the finding by [10] (explained in §II-B), we propose to use a single speaker’s EMA as a template articulatory space to represent speaker-generic articulatory kinematics. We selected one of the largest single-speaker EMA datasets, MNGU0 [50], that includes 75 minutes of EMA collected while reading newspapers aloud. This dataset is widely accepted and verified in many studies, given a fine signal quality carefully controlled by the authors. We claim all speakers’ articulations can be represented on this single-speaker EMA space without losing information that contributes to the intelligibility of speech. That is, EMA represents phonetic content in a way that can be detached from the variance of vocal tract anatomical structure across individuals. Our results show empirical evidence of this claim.

We use the SSL-linear AAI approach proposed by [9], [10]. The SSL-linear model is built by training a linear mapping from SSL features to EMA, while keeping the SSL encoder weights frozen. This simple mapping can effectively find a linear subspace in the SSL feature space which is highly correlated with EMA, proven by previous probing studies [9], [10]. We use the WavLM Large model [51], which shows the highest correlation amongst speech SSL models as reported in [9]. Note that the linear head is the only fitted part here,

thus, maintaining the generalization capacity of the WavLM encoder that is attained by pretraining on large-scale speech data and adversarial data augmentation [51]. Furthermore, the speaker information tends to diminish after a few early layers [48], which indicates the mapping can be speaker-agnostic, further contributing to multi-speaker generalizability.

The original 200 Hz EMA data is downsampled to 50 Hz to match the sampling rate of the SSL features, and z-scored within utterances. A low-pass filter is applied to the features to remove high-frequency noise, where the frequency threshold is set as 10 Hz. We used the 9th layer of the WavLM Transformer encoder from which the features are extracted for inversion (see Appendix A.1 for the selection procedure). The resulting AAI model outputs 12 channels of EMA (X and Y axis of each of 6 articulators) with 50 Hz frequency.

2) *Source Features*: Though EMA has a full descriptive capacity of the place of articulation, it lacks source information generated by the glottal excitation, which is crucial to implementing the manner of articulation and expressing the prosody of speech. Therefore, we include pitch (or fundamental frequency (f_0)) and loudness features to represent the source features [18], [19], [52]. The loudness feature also informs non-larynx constriction, which is important for voiced fricatives such as “z” and “v”. We use CREPE [53] to infer pitch from speech, and loudness is measured by the average of absolute magnitudes of waves for every 20 ms. Together with the EMA from AAI, we referred to these features as “articulatory features” that have 14 channels (12 EMA + 2 source) and a 50 Hz sampling rate.

3) *Speaker Identity*: Though we rule out the individual variance in vocal tract anatomy by using a template space, such missing anatomical configuration is an important determinant of the voice texture, or timbre, of an individual speaker which is a crucial factor in defining the speaker’s identity [54]. Note that our definition of the speaker identity does not include information about dialect or accent which is actually aimed to be

TABLE I
COMPARISON OF MULTI-SPEAKER AAI SYSTEMS. PERFORMANCE IS MEASURED AS PEARSON CORRELATION COEFFICIENT (PCC).

System	Model	Dataset	
		MOCHA	HPRC
Tract Variable	Wu et al. [17]	0.678	0.784
	Siriwardena & Espy-Wilson [28]	–	0.757
Single-speaker	Ours	0.739 ± 0.017	0.761 ± 0.012

disentangled from the speaker identity. Here, we compensate for this missing information with a separate speaker identity encoder which is jointly trained with a vocoder to extract the speaker-specific speaker information.

To this end, we propose a simple yet effective speaker encoder, which minimizes the trainable portion of the model. Based on the observation by [48], [55] that the speaker information is largely concentrated in the CNN outputs of speech SSL models, the encoder consists of the frozen CNN extractor from WavLM Large followed by a weighted pooling layer and a learnable feedforward network (FFN). The pooling layer weighted-averages the acoustic features from WavLM CNN across frames, where the weight is given by the periodicity inferred from CREPE. This allows more attention to the periodic signals which may encode voice texture better, and rules out non-speech frames. Then, the FFN projects the average feature to a speaker embedding with 64 channels. This speaker identity encoding is indispensable to fully map out multi-speaker speech.

B. Articulatory Synthesis

We adopt HiFi-GAN as the vocoder for articulatory synthesis [56], [14], [44]. The vocoder is trained to synthesize speech audio with a 16K Hz sampling rate from articulatory features defined in §III-A1 and §III-A2. To condition the generation on the speaker embedding, we apply FiLM [57] to each convolution module with different receptive fields in the HiFi-GAN architecture, which modulates the output channels of each module. We adopt the same loss functions as [56]: Mel-spectrogram loss for reconstruction and multi-period and multi-scale discriminator loss for GAN training.

C. Dataset

For training the vocoder, we use LibriTTS-R [58], an enhanced version of LibriTTS [59]. The dataset is comprised of 585 hours of reading audiobooks ((555, 15, 15) hours for (train, dev, test) sets). The original 24K Hz audio is downsampled to 16K Hz. We use VCTK [60] to further evaluate the generalizability of the model to a broader range of speakers and accents. The entire VCTK dataset is not included in the training set and is only used for evaluation.

Note that only the FFN in the speaker identity encoding and the vocoder are updated in the large-scale training (orange modules in Fig. 2), and the rest of the pipeline remains fixed while training. More details of implementation and training are in Appendix B.1-7.

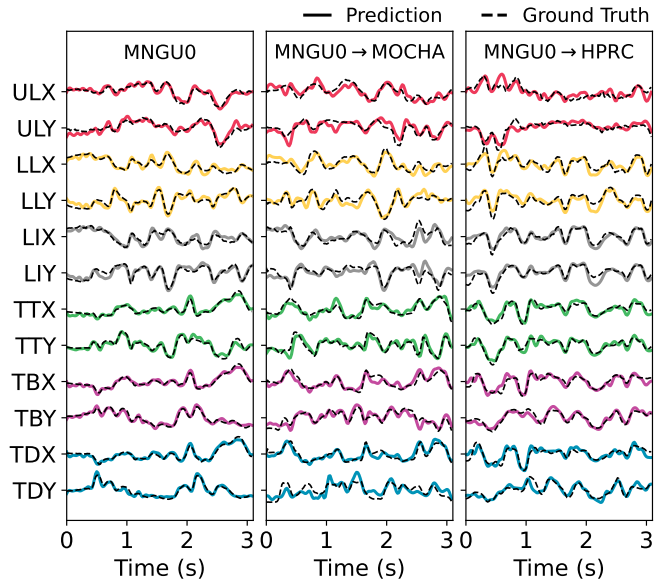


Fig. 3. Examples of SSL-linear prediction on MNGU0 (left), transformed prediction from MNGU0 to a female MOCHA speaker (middle) and to a male HPRC speaker (right). Predictions are denoted with the colored lines and ground truths are denoted with the black dotted lines.

IV. RESULTS & EXPERIMENTS

We evaluate the proposed articulatory encoder in different aspects to validate each part of the framework – universality of articulatory encoding, IV-A, information conservation in encoding-decoding (or resynthesis) IV-B, and disentanglement of speaker embedding by speaker identity encoding IV-D.

A. Universality of Single-Speaker Articulatory Encoding

As we claim a single-speaker AAI can be used for universal articulatory encoding, we compare our model with the existing state-of-the-art (SOTA) multi-speaker articulatory encoding systems that utilize tract variables [17], [28]. The tract variables are a set of articulatory parameters that can be derived from EMA and are known to be more regularized across speakers [61]. Table I denotes the performance of the tract-variable-based AAI systems and ours on two multi-speaker EMA datasets, MOCHA [62] and HPRC [63]. MOCHA includes 7 speakers with 27 minutes of data per speaker on average, and HPRC includes 8 speakers with 59 minutes of data per speaker on average. The performance is evaluated by the Pearson correlation coefficient (PCC), where results besides ours are retrieved from reference papers (95% confidence interval is denoted for our case.). Since our AAI is trained on a single-speaker (MNGU0) articulatory space, we fit a linear model that maps the MNGU0 articulatory space to another speaker’s articulatory space to measure the correlation [10]. As a result, our single-speaker AAI system shows correlations higher in MOCHA and slightly lower in HPRC compared to Wu et al. [17], and slightly higher in HPRC compared to Siriwardena and Espy-Wilson [28]. Note that this is not a fair comparison since the scores are measured on different variables. However, this system-wise comparison suggests that the single-speaker approach can yield a similar

TABLE II

PERFORMANCE COMPARISON OF GROUND TRUTH SPEECH (GT) AND RESYNTHEZIZED SPEECH BY ARTICULATORY ENCODEC (RESYNTH)

Dataset	Input	Intelligibility		Quality	
		WER↓	CER↓	MOS↑	UTMOS↑
LibriTTS-R	GT	4.22	2.24	4.01 ± 0.16	4.10 ± 0.58
	Resynth	5.43	2.90	3.82 ± 0.20	4.12 ± 0.58
VCTK	GT	1.66	0.74	3.65 ± 0.16	3.84 ± 0.54
	Resynth	3.73	1.96	3.67 ± 0.17	3.95 ± 0.52

level of consistency across multiple speakers. Moreover, our approach only fits a linear model, thus it is likely to be more generalizable than the previous systems which use non-linear, deep recurrent neural networks. Fig. 3 demonstrates prediction examples of the predicted EMA. The left panel shows a near-perfect prediction even with a simple linear mapping from WavLM, and even after the affine transformation from MNGU0 space to other speakers, the predictions show high correlations with the ground truths (middle and right panel). The prediction performance on MNGU0 shows 0.878 ± 0.012 average correlation (see Appendix A.2-4. for more analyses).

B. Performance of Resynthesis by Articulatory Encodec

We evaluate the performance of the articulatory encodec in terms of intelligibility and quality of resynthesized speech audio. We used an out-of-the-box automatic speech recognition (ASR) model, Whisper ("openai/whisper-large-v3"), to evaluate the word error rate (WER) and character error rate (CER) of resynthesized speech.³ The quality of the audio is measured by a human-evaluated subjective metric, mean opinion score (MOS), and a machine-evaluated MOS, UTMOS [64]. We evaluate both ground truth speech and resynthesized speech on the test-clean subset of LibriTTS-R which includes 8.56 hours from 39 unseen speakers. To further evaluate the generalizability of the model, we evaluate the model on VCTK data which includes 107 speakers with 500 utterances in total. Table II summarizes the performance in comparison with the ground truth speech. For the quality metrics, we reported 95% confidence intervals. When tested on LibriTTS-R, the ASR on the resynthesized speech shows high intelligibility with WER of 5.43% and CER of 2.90%, which is marginally different from those on the ground truth. Moreover, our articulatory synthesis generates natural speech sounds showing decent quality with MOS of 3.82 which is a 0.19 decrease from the ground truth, and with UTMOS of 4.12 which is on par with the ground truth.

Furthermore, the results on VCTK also demonstrate high intelligibility with WER of 3.73% and CER of 1.96%. Though the gap from the ground truth is larger than LibriTTS-R, this is a remarkable level of performance given that the model is not exposed to the entire dataset during training. As the training set audio corpus which has cleaner audio than VCTK, the model demonstrates some speech enhancement capacity which results in a higher MOS and UTMOS than the ground truth. While the speakers in LibriTTS-R are concentrated on American English, VCTK includes a variety of accents, primarily

³The transcription is normalized before measuring the error rates.

TABLE III

INTELLIGIBILITY OF MULTILINGUAL APPLICATION. WER AND CER ON GROUND TRUTH SPEECH (GT), RESYNTHEZIZED SPEECH BY ENGLISH-ONLY TRAINED MODEL (EN-R), AND BY MULTILINGUAL MODEL (ML-R).

Language	WER↓			CER↓		
	GT	EN-R	ML-R	GT	EN-R	ML-R
German	5.23	15.32	9.70	1.89	6.66	3.95
Dutch	9.90	20.20	15.39	2.82	8.83	5.70
Portuguese	7.10	17.81	12.80	2.19	8.50	5.21
Italian	9.63	22.09	15.53	2.43	7.40	4.98
Polish	4.19	14.79	9.89	0.94	4.63	2.87
Spanish	3.96	10.74	6.79	1.26	4.73	2.38
French	4.62	16.67	8.04	2.65	9.90	4.54
Korean	6.31	15.88	13.66	1.01	6.72	4.96
Japanese	–	–	–	5.65	8.45	8.16
Chinese	–	–	–	10.69	31.27	23.28
Average	6.37	16.69	11.48	3.15	9.71	6.60
w/o Chinese	6.37	16.69	11.48	2.32	7.31	4.75

focusing on English speakers with different regional accents from the United Kingdom. Therefore, the high performance demonstrated on VCTK suggests that the articulatory encodec can robustly generalize to unseen speakers and accents.

C. Multilingual Application

We evaluate the articulatory encodec on speech corpora from other languages: 7 European languages (German, Dutch, Portuguese, Italian, Polish, Spanish, French) from multilingual LibriSpeech [65] and 3 East Asian languages (Korean, Japanese, and Chinese (Mandarin)) from KSS [66], JVS [67], and AISHELL [68], respectively. Except for KSS, all corpora include multiple speakers. We randomly sampled 200 utterances from the test split of each corpus to evaluate the intelligibility of resynthesized speech.⁴ Table III compares WER and CER by ASR (Whisper) in each language. As no space is used for Japanese and Chinese, we omit the WER for these languages. We also evaluate the performance of a version of the model that is fine-tuned to the multilingual data, which is denoted as ML-R in Table III). The original English-only trained encodec is denoted as EN-R. See Appendix B.8. for details of the fine-tuning procedure.

As shown in Table III, with only training in English, the resynthesis by articulatory encodec achieves average WER of 16.69 excluding Japanese and Chinese, average CER of 9.71. Roughly, if the conflated Chinese CER is excluded, the EN-R preserves a fair amount of information given that 93% of characters are correctly recognizable. Despite huge gaps from the ground truth observed, this is remarkable generalizability given both encoding and decoding procedures have only seen English in training. When fine-tuned, the average WER and CER are cut down to 11.48% and 6.60%, respectively. This indicates that some portion of the errors is induced by the out-of-domain application of the vocoder, thus fine-tuning is able to yield a huge gain in performance. Yet, there are unresolved gaps from the ground truth, which would be attributed to the fact that we are only tuning the vocoder and keeping the encoder part intact. This is also aligned with the observation that there is a slight language bias in the articulatory representation in SSL [10].

⁴We excluded samples with numbers to avoid converting Arabic numerals.

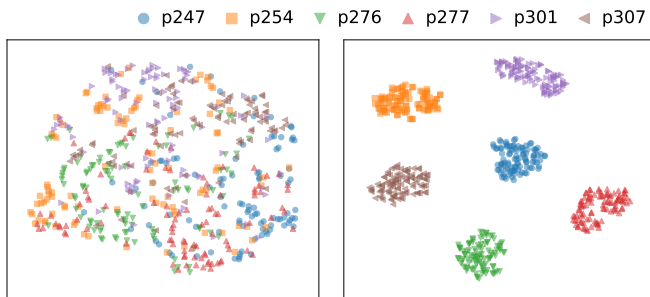


Fig. 4. Visualization by T-SNE of utterance-wise averaged articulations (left) and speaker embeddings (right) from 6 different VCTK speakers. The perplexity is set as 10.

TABLE IV
FEW-SHOT SPEAKER IDENTIFICATION ACCURACY (SID ACC). FOR VCTK, THE ACCURACY OF FULL-TRAIN DATA TEMPLATE EMBEDDINGS IS DENOTED IN PARENTHESES.

Model	SID ACC (%) [†]	
	LibriTTS-R	VCTK
x-vector	91.7	83.4 (88.2)
r-vector	98.3	99.8 (99.8)
Ours	95.5	92.2 (94.6)

D. Speaker Recognition and Voice Control by Speaker Identity

The speaker identity encoding is especially important to inform voice texture for speech synthesis since the proposed articulatory encoding is agnostic to speakers. On one hand, this suggests that the model can learn a speaker embedding that is disentangled from individual articulatory patterns, or dialects and accents. Here, we evaluate this claim by experiments on few-shot speaker identification and zero-shot voice conversion.

First, we build a few-shot, learning-free speaker identification (SID) by comparing the similarity between the speaker embeddings. For each test speaker, 10 first clips in the dataset are concatenated and then the template speaker embedding for the speaker is extracted. Then among the potential test speakers, the speaker is identified as the speaker with maximal similarity in the template and tested speaker embedding. For LibriTTS-R, we use speakers in the test-clean set with at least 10 clips, leaving 36 speakers. For VCTK, we use the train set clips to create the template embeddings for 107 test speakers. Additionally, we also evaluate SID accuracy using all data in the train set for creating the templates, which is denoted in parentheses in Table IV.

Our speaker encoding shows high discriminability in the few-shot SID, achieving 94.7% accuracy in LibriTTS-R and 92.2 % accuracy in VCTK test sets. When all utterances in the train set are used, the accuracy for VCTK reaches 94.6 %. Our embedding outperforms the widely adopted speaker embedding, x-vector [69] by a large margin, especially in VCTK which is a harder case with a larger number of speakers (Table IV).⁵ As a sanity check for the proposed SID task, we evaluate the accuracy with the current state-of-the-art speaker embedding, ResNet based r-vector by WeSpeaker [70], which

shows a near-perfect SID accuracy.⁶ However, the r-vector embedding is extracted from very deep ResNet with 221 layers, which is way larger than ours and x-vector, therefore the model may incorporate more speaker information than voice texture (e.g., dialect and accent). Both x-vector and r-vector models are trained on VoxCeleb corpus [71], [72], [73]. Overall, this suggests that our speaker encoding can extract highly discriminable features for speaker identification.

We further evaluate the validity of our identity encoding by zero-shot voice cloning application. We selected 6 speakers from VCTK, where their mean pitch values are equidistant in the range from 80 Hz to 230 Hz. Fig. 4 visualizes the speaker embedding of the selected speakers, demonstrating that each speaker’s utterances are clustered distinctively. On the contrary, no speaker-relevant cluster is identifiable in the manifold of utterance-wise averaged articulations, indicating disentanglement between articulation and speaker identity. For each target speaker, the first 10 clips in the training set are concatenated and then the speaker embedding is extracted. Then, the voice from the source speaker is converted by switching speaker embedding in the resynthesis. Additionally, the pitch range of the source speaker is adjusted to match that of the target speaker, by z-scoring the source pitch trace; and shifting and rescaling to match the center and scale of the target pitch range (“P-rescale”). We convert all audio clips in test-clean set of LibriTTS-R with more than 2 seconds of duration, to each of 6 VCTK target speakers.

We evaluate “coding-recoding similarity” of the voice-converted speech. The coding-recoding similarity measures the correlation between the original input speech coding and the encoding of the output of the articulatory synthesis, where the voice is controlled. For articulation, we measure the Pearson correlation of each of 12 channels and then average them, and for pitch and loudness, the correlation is separately reported. For speaker identity, the cosine similarity between the conditioning target embedding and that of the generated speech. Furthermore, we report the SID accuracy based on the task designed in the above few-shot SID, and WER and UTMOSto check the intelligibility and quality of the converted audio. As baselines, we evaluate existing voice conversion models: YourTTS [74], a multi-speaker TTS that offers zero-shot voice conversion, and QuickVC [47], an SSL-based encodec model which conditions voice on an acoustics-based speaker encoding. The former is included as an example of a voice conversion with text-prior, and the latter is included since the model has a similar SSL-based encoding but without the articulatory constraint.⁷ Furthermore, we evaluate the coding-recoding similarity of the self-targeted resynthesized speech (“Ours-Resynth” in Table. V). The results are summarized in Table. V with 95% confidence intervals if applicable.

As a result, the voice-converted speech by the articulatory encodec can be accurately identified as the target speaker among 107 VCTK speakers, achieving 94.6 % SID accuracy (Table. V). Though the speaker coding-recoding similarity is

⁵We retrieved checkpoints from <https://huggingface.co/speechbrain/spkrec-xvect-voxceleb>.

⁶We use “resnet221_LM” checkpoint from <https://github.com/wenet-e2e/wespeaker>.

⁷Up to our knowledge, this is the only open-sourced SSL-based encodec with an official checkpoint.

TABLE V
PERFORMANCE COMPARISON OF ZERO-SHOT VOICE CONVERSION

Model	Target Spk	Coding-Recoding Similarity (PCC)				SID \uparrow	WER \downarrow	UTMOS \uparrow
		Articulation \uparrow	Pitch \uparrow	Loudness \uparrow	Speaker \uparrow			
YourTTS	VCTK	0.923 \pm 0.021	0.881 \pm 0.165	0.881 \pm 0.062	0.817 \pm 0.080	81.4	4.00	4.05 \pm 0.51
QuickVC	VCTK	0.930 \pm 0.021	0.868 \pm 0.172	0.903 \pm 0.063	0.831 \pm 0.070	66.7	4.17	4.22 \pm 0.36
Ours	VCTK	0.944 \pm 0.015	0.944 \pm 0.093	0.938 \pm 0.037	0.879 \pm 0.069	94.6	4.83	3.83 \pm 0.58
w/o P-rescale	VCTK	0.943 \pm 0.016	0.894 \pm 0.150	0.929 \pm 0.045	0.791 \pm 0.100	73.9	4.82	3.77 \pm 0.78
Ours-Resynth	Self	0.954 \pm 0.014	0.968 \pm 0.109	0.936 \pm 0.077	0.962 \pm 0.038	91.5	4.40	4.00 \pm 0.59

lower than the self-targeted resynthesis (0.879 and 0.962, respectively), the SID result suggests that this level of similarity is high enough to be discriminable from more than a hundred unseen speakers. Furthermore, our approach shows higher SID accuracy than both of the baseline models, where the speaker coding-recoding similarities are also inferior to ours.

The SID accuracy and the coding-recoding similarity of pitch and speaker identity significantly drop when we ablate the pitch rescaling (“w/o P-rescale” in Table. V), indicating an interplay between pitch range and speaker identity encoding. This may be induced by the natural correlation between speaker identity and pitch range, which is likely to be confounded by biological sex. However, the coding-recoding similarity of articulation and loudness remains intact, showing a marginal difference from the pitch-rescaled voice conversion.

The high coding-recoding similarity in articulation suggests that the articulation is well disentangled from speaker identity and pitch, which indicates that the dialect is preserved after the voice conversion. The correlation is as high as 0.944 and is marginally different from the self-targeted resynthesis, 0.954, which also indicates the stability of the coding by our articulatory encoder. This result further supports that the proposed AAI is agnostic to speaker identity. Moreover, the similarities outperform baselines, especially in pitch, suggesting our model better disentangles the pitch. Lastly, the intelligibility slightly decreases after the voice conversion, but the difference is marginal and the speech remains highly intelligible with WER of 4.83 %. The YourTTS converted speech shows a lower WER of 4.00 %, which might be driven by the text-to-speech (TTS) prior in the model. Finally, the voice conversion shows some degraded UTMOS as 3.83, 0.17 decrease compared to the resynthesis, and QuickVC shows the highest UTMOS as 4.22. This suggests that our model has a potential trade-off between disentanglement and audio quality of the synthesized audio. However, this degrades in naturalness may be confounded by a natural correlation between accents and voice textures, so that some voice conversion cases may result in rare combinations of accent and speaker identity, harming the UTMOS score. To sum up, the articulatory encoder is a stable and disentangled coding system of speech.

V. DEMONSTRATION OF INTERPRETABILITY AND CONTROLLABILITY OF ARTICULATORY ENCODEC

Unlike other high-dimensional neural coding, the proposed articulatory coding is highly interpretable and controllable. Interpretability is naturally granted by having a low-dimensional coding space, where each dimension corresponds to the physical articulator on the vocal tract. Furthermore, as the vocal

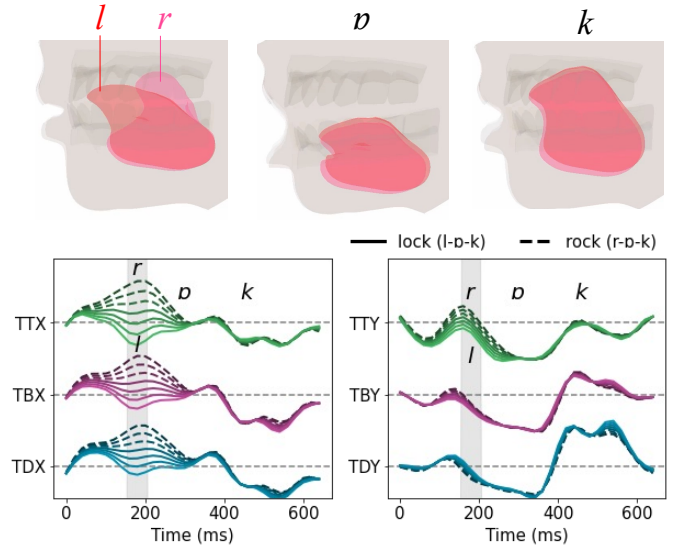


Fig. 5. Articulatory traces encoded for speaking “lock” and “rock”, denoted by the different line styles, “-” and “- -”, respectively. The bottom panel shows the midsagittal displacements of TT, TB, and TD, and the top panels show snapshots of the corresponding vocal tract anatomy. In the snapshots, the vocal tract of “lock” and “rock” are overlaid with separate colors, orange and pink, respectively. The shaded region indicates the window of “l” or “r”. The color is darkened while interpolating from “lock” to “rock”, where the line style again indicates the recognized words.

tract articulation is the control space of speech production, the encoded articulatory features can be controlled with the same principle as how we produce speech. The control or modification of articulatory features then can be played back by the vocoder which functions as a physical simulation of the vocal tract articulation [3], [75], [12], [40], [16]. Here, we demonstrate these features with two cases.

A. Case 1: Place of Articulation – “lock” vs “rock”

The first case is about demonstrating how the articulatory encoder can be used to interpret and control the place of articulation in speech. Here, we select two speech clips of speaking “lock (l-D-k)” and “rock (r-D-k)” as an example showing the difference between alveolar and post-alveolar approximants. The encoded articulatory traces of these two words are depicted in Fig. 5, along with snapshots of vocal tract anatomy. The encoded traces and 2D visualization offer an intuitive interpretation of how the vocal tract is dynamically shaped while speaking. Furthermore, this successfully highlights the known phonological distinction between these

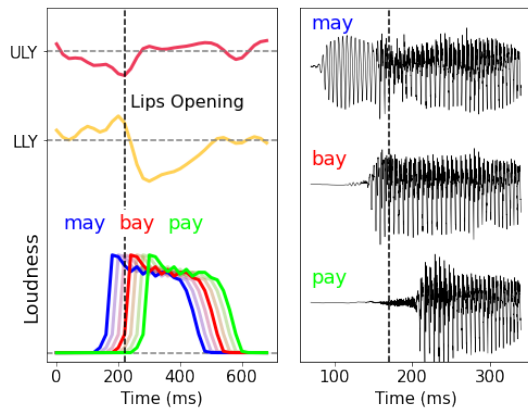


Fig. 6. Articulatory modulation example for “bay”. The left panel shows the Y axis of UL and LL with the vertical dashed line indicating the beginning of the lips opening. The loudness trajectories are depicted, which are moved back and forth, while the salient red, green, and blue colors indicate the perceived plosives. The right panel shows zoom-in wave form of synthesized audio around the lips opening, showing the different voice onset times.

two approximants: “*r*” approximates tongue to a more anterior part of the palate (alveolar) than “*r*” (post-alveolar).

We further demonstrate the simulated control by interpolating tongue articulations between the words [14]. The mixing factor, α , is applied to weigh the sum of each of the tongue articulatory traces (TT, TB, and TD), i.e., $Art(\text{“lock”}) \cdot \alpha + Art(\text{“rock”}) \cdot (1 - \alpha)$. The Fig. 5 bottom panel shows the interpolated traces with $\alpha \in \{1.0, 0.8, 0.6, 0.4, 0.2, 0.0, -0.2\}$, gradually changing pronunciation from “lock” to “rock”. Then, ASR is applied to determine which word is perceived, drawing a perceptual boundary between the interpolation at $\alpha = 0.2$, which is denoted as a separate line style in Fig. 5. This demonstration shows that the articulatory encoder provides interpretable control knobs, which can be manipulated to simulate speech sounds and observe the causal interaction between articulatory control and the generated speech.

B. Case 2: Manner of Articulation – Voice Onset Time

The next example is about the manner of articulation, especially focused on the phonological phenomena called voice onset time (VOT). While the spatial arrangement of articulators forms the filter that shapes the consonants, the manner of sound further categorizes the consonants into some perceptually distinguishable sounds. In this example, we demonstrate that the VOT can be directly implemented by the timing of the rise of loudness.

Here, a speech clip saying “bay” is encoded by the articulatory encoder (Fig. 6 left). We only show the traces of lips on the Y axis as these are the key articulatory factors of labial consonants. We can clearly see the lips opening around 200 ms. Then, we shift the loudness trace back and forth and generate speech from the manipulated features. By shifting the loudness trace 60 ms earlier than the moment of lips opening, we can nasalize the sound from “bay” to “may” (from plosive to nasal). On the other hand, by shifting it 60 ms backward, the sound is converted to “pay” (from lenis plosive to fortis plosive). We can also observe the induced VOT difference

along this manipulation (Fig. 6 right), which is aligned with the known VOT patterns of nasal and plosive sounds.

These two proof-of-concept showcases suggest the promising utility of the articulatory encoder as a physical simulator of articulatory control, and as a speech analysis tool that provides a natural and intuitive phonological interpretation.

C. Potential Applications

We list some examples of potential applications here. First, the framework can be used as an analysis platform for investigating a phonological basis of speech without collecting high-cost articulatory data [16]. Second, the high-performance synthesizer can be used as a speech simulator, which can facilitate a control theoretic approach to speech processing or reinforcement learning of speaking agents [3], [76], [40], [77]. Third, the universal articulatory encoding can be utilized for a language learning tool or therapy, where looking through the vocal tract can aid the learning experience [78], [79], [80]. Lastly, a TTS system can be built upon the articulatory encoder that synthesizes articulatory control from text or higher-order structure of speech [81], [82], [83]. This can reveal a descriptive and interpretable relationship between text and articulation. To conclude, our framework has promising utilities in various domains in both speech science and engineering.

VI. CONCLUSION

We propose a novel encoding-decoding framework of speech, *articulatory encoder*, which mimics the biophysical interface of speech production. By projecting speech to articulatory features, the speech can be expressed in a low-dimensional space, where each channel corresponds to an articulator on the vocal tract. Such physical embodiment of speech coding enables a natural, intuitive interpretation, which is further facilitated by a visual aid that displays the articulation in a 2D animation. With large-scale training, our proposed articulatory encoder achieves a high-performance articulatory resynthesis that can generalize to unseen speakers and novel dialects, with a minimal loss of information compared to ground truth speech. To our knowledge, this is the first demonstration of universal articulatory synthesis that can scale up to an indefinite number of speakers. This universality is aided by a novel speaker identity encoding, which embeds highly discriminable speaker-specific speaker. Furthermore, the encoded speaker embedding is effectively disentangled from articulatory features and can be used for accent-preserving voice conversion.

In future work, we will scale the articulatory encoder to incorporate expressive speech and singing. Also, we will improve the robustness of the system under noisy environments. These efforts will maximize the promising utilities of the articulatory coding of speech.

ACKNOWLEDGEMENTS

This research is supported by the following grants to PI Anumanchipalli — NSF award 2106928, BAIR Commons-Meta AI Research, the Rose Hills Innovator Program, UC

Noyce Initiative, at UC Berkeley, and Google Research Scholar Award.

APPENDIX A – ADDITIONAL ANALYSIS

A.1. Layer-wise AAI Performance

We selected the 9-th layer after comparing the inversion performance of each layer measured by Pearson correlation coefficients (PCC) averaged across EMA channels on 5-fold cross-validation (Fig. 7). For each fold, 100 test utterances are randomly held out and 95 % confidence intervals are denoted. At the best layer (the 9th), the average correlation is 0.878 ± 0.012 . After the layer selection, all data from MNGU0 are used to fit the linear model.

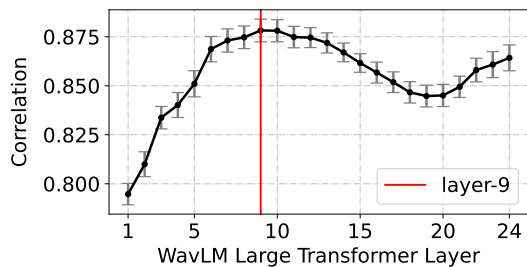


Fig. 7. Probing performance of each layer in WavLM Large on MNGU0

A.2. AAI Performance on Individual Articulator

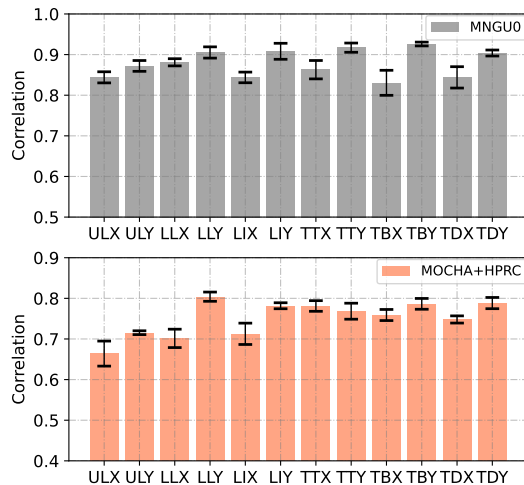


Fig. 8. Correlation of individual channels on MNGU (top) and other speakers in MOCHA and HPRC (bottom).

The performances of AAI on the individual channels are denoted in Fig. 8, measured by correlation (PCC) with 95 % confidence intervals. The top pannel shows performance on MNGU0 and the bottom channel shows performance after the transformations to other speakers (15 speakers from MOCHA+HPRC). In both cases, the Y-axis traces are generally better predicted than the X-axis traces.

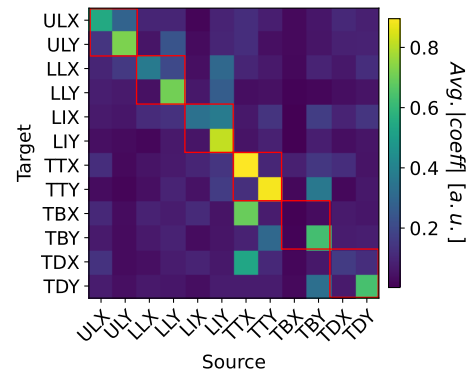


Fig. 9. Average absolute coefficients of affine transformation from MNGU0 to other speakers.

A.3. Evidence of Geometric Isometry Between Individual Articulatory Space

As shown in [10], the weights of the linear transformations across speakers are highly concentrated within the articulators (Fig. 9; red diagonal boxes). The tongue tip is also affected by the tongue blade and dorsum, which is natural since the tongue is connected and sensor positions are not firm, but still significantly more affected by the tongue tip.

A.4. Evidence for Excluding Coronal Axes of EMA

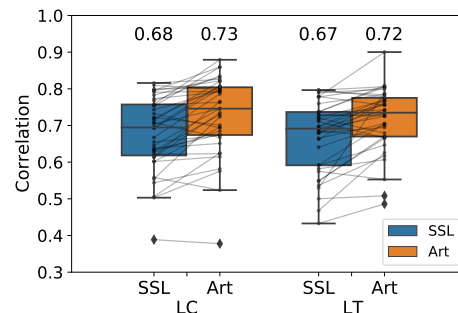


Fig. 10. Linear probing on the coronal axis of the left corner of the mouth (LC) and the lateral tongue (LT). The prediction performance by using WavLM features (SSL) and 12 other midsagittal articulatory channels (Art). Each dot is a speaker.

In our aritulatory encoding, we largely ignore the coronal axes of EMA data. Here, we provide evidence for such exclusion with a probing analysis. The same linear probing is conducted using SSL features (WavLM) and the original 12 midsagittal articulatory channels. We use EMA-MAE [84] for this experiment since the dataset includes two coronal channels: the left corner of the mouth (LC) and the lateral tongue (LT). Both for LC and LT, the linear probing using SSL features is significantly worse than using articulatory features (for LC, SSL features: 0.68 ± 0.19 , articulatory features: 0.73 ± 0.20 ; for LT, SSL features: 0.67 ± 0.19 , articulatory features: 0.72 ± 0.17). This suggests that those coronal features can be predicted with a fair correlation (0.72-0.73) by a linear combination of the existing 12 channels. These results suggest

that the coronal axes can be safely ruled out for the proposed encodec framework.

APPENDIX B – MODEL & TRAINING DETAIL

B.1. Pitch Tracker Configuration

For CREPE, we use a PyTorch implementation called “torchcrepe”⁸. We use “full” model and the range of pitch is set as from 50 to 550. The default Viterbi decoding is used. The input waveform is resampled to 16K Hz and z-scored within the utterance. We found that if we set the hop length as 320 to output 50 Hz (the sampling rate of SSL features), sometimes, it makes errors in some female speakers with high pitch levels. To mitigate that we decrease the hop length to 80 which results in 200 Hz outputs, and then, we downsample the output pitch and periodicity by a factor of 4 to match the 50 Hz sampling rate. As a side effect, we observe that the periodicity is sometimes erroneously detected with such hop length modification. Therefore, we threshold the periodicity bigger than 0.4. The periodicity thresholding is only applied for the inference time.

B.2. Loudness Implementation

The loudness is estimated as the average of the absolute magnitude of the input waveform for every 20ms bin. This is implemented with a fixed, single-channel convolutional layer with a stride of 320 and kernel size of 320, where each weight in the kernel is set as 1/320. Likewise, the waveform is resampled to 16K Hz and z-scored within utterance.

B.3. Speaker Identity Encoder Architecture

The CNN outputs of WavLM Large are weighted by periodicity inferred from CREPE and averaged across frames per utterance. Here, we also include the convolutional positional encoding and the projection layer applied for the CNN outputs, in the original WavLM model. That is, we use the features right before entering the Transformer encoder, which has 1024 channels. The FFN is composed of a linear layer that maps 1024 input features to 1024 output features, followed by GELU and dropout with 0.2, and then another linear layer that projects features to 64-channel speaker embedding. This FFN is the only network trained within the vocoder training and other parts are not updated.

B.4. Generator Architecture

Following the HiFi-GAN architecture, our generator is a convolutional neural network composed of transposed convolutions each followed by a multi-receptive field fusion (MRF) module [56]. Each MRF module outputs the sum of three residual block outputs [85]. For our three residual blocks, we use dilations of 1, 3, and 5 and kernel sizes of 3, 7, and 11, respectively. For our transposed convolutions, we use kernel sizes of 10, 8, 4, and 4, and each stride is half the respective kernel size. Channels are halved each layer until the final layer outputs a single channel corresponding to the acoustics.

To condition the generation on speaker identity, a FiLM layer is applied for outputs of each residual convolutional layer in the MRF module [57]. Every FiLM layer is implemented as a linear layer followed by ReLU and dropout of 0.2, and another linear layer to predict scale and center for each channel of the targeted convolution outputs. These scales and centers are then multiplied and added to the outputs of convolutional layer that the FiLM layer is attached to (feature-wise affine transform).

B.5. Discriminator Architecture

We utilize two types of discriminators as in the HiFi-GAN model: (1) a multi-period discriminator (MPD), and (2) a multi-scale discriminator (MSD) [56]. The MPD takes as input evenly-spaced input frames, and the MSD average-pools the input. Then, both models feed the processed inputs into convolutional neural networks (CNNs). We follow the same CNN architectures as the HiFi-GAN discriminators [56]. Each MPD CNN is composed of strided convolutional layers each followed by leaky rectified linear unit (ReLU) activation functions. Similarly, each MSD CNN is composed of strided and grouped convolutional layers each followed by leaky ReLUs. Like HiFi-GAN, we use five MPDs with spacings of 2, 3, 5, 7, and 11, and three MSDs that rescale inputs by 1, 2, and 4 times.

B.6. Loss Configuration

Like HiFi-GAN, our loss function is a weighted sum of the GAN loss, mel-spectrogram loss, and feature matching loss [56]. The weight for three loss terms are 1, 45, and 2, respectively. For the mel-spectrogram loss, we use the following parameters: {fs: 16000, fft_size: 1024, hop_size: 160, win_length: null, window: "hann", num_mels: 80, fmin: 0, fmax: 8000}.

B.7. Training Detail

We use Adam optimizer with learning rate of 10^{-4} and beta of (0.5, 0.9). The model is updated for 1.5M iterations, and the learning rate is halved by every 8K steps which stays static after 320K steps. For every iteration, a random 320 ms window is sampled from each clip in a batch with a size of 64.

B.8. Multilingual Fine-Tuning Detail

We fine-tune the model on the multilingual datasets for 500K iterations. The model is initialized with a checkpoint of the model trained only on English for 1M iterations. The training data include 555 hours of English, 1965 hours of German, 1553 hours of Dutch, 161 hours of Portuguese, 247 hours of Italian, 104 hours of Polish, 917 hours of Spanish, 1075 hours of French, 60 hours of Chinese, 22 hours of Japanese, and 11 hours of Korean. The English proportion is the train split of LibriTTS-R.

⁸Retrieved from <https://github.com/maxmorrison/torchcrepe>.

REFERENCES

- [1] T. Chiba and M. Kajiyama, *The vowel, its nature and structure*. Phonetic society of Japan, 1958.
- [2] G. Fant, *Acoustic theory of speech production: with calculations based on X-ray studies of Russian articulations*. Walter de Gruyter, 1971, no. 2.
- [3] S. Maeda, "Compensatory articulation during speech: Evidence from the analysis and synthesis of vocal-tract shapes using an articulatory model," in *Speech production and speech modelling*. Springer, 1990, pp. 131–149.
- [4] C. P. Browman and L. Goldstein, "Articulatory phonology: An overview," *Phonetica*, vol. 49, no. 3-4, pp. 155–180, 1992.
- [5] I. P. Association, *Handbook of the International Phonetic Association: A guide to the use of the International Phonetic Alphabet*. Cambridge University Press, 1999.
- [6] J. Chartier, G. K. Anumanchipalli, K. Johnson, and E. F. Chang, "Encoding of articulatory kinematic trajectories in human speech sensorimotor cortex," *Neuron*, vol. 98, no. 5, pp. 1042–1054, 2018.
- [7] G. K. Anumanchipalli, J. Chartier, and E. F. Chang, "Speech synthesis from neural decoding of spoken sentences," *Nature*, vol. 568, no. 7753, pp. 493–498, 2019.
- [8] C. J. Cho, E. Chang, and G. Anumanchipalli, "Neural latent aligner: cross-trial alignment for learning representations of complex, naturalistic neural data," in *International Conference on Machine Learning*. PMLR, 2023, pp. 5661–5676.
- [9] C. J. Cho, P. Wu, A. Mohamed, and G. K. Anumanchipalli, "Evidence of vocal tract articulation in self-supervised learning of speech," in *ICASSP 2023-2023 IEEE International Conference on Acoustics, Speech and Signal Processing (ICASSP)*. IEEE, 2023, pp. 1–5.
- [10] C. J. Cho, A. Mohamed, A. W. Black, and G. K. Anumanchipalli, "Self-supervised models of speech infer universal articulatory kinematics," 2024.
- [11] W.-N. Hsu, B. Bolte, Y.-H. H. Tsai, K. Lakhotia, R. Salakhutdinov, and A. Mohamed, "Hubert: Self-supervised speech representation learning by masked prediction of hidden units," *IEEE/ACM Transactions on Audio, Speech, and Language Processing*, vol. 29, pp. 3451–3460, 2021.
- [12] P. Birkholz, "Modeling consonant-vowel coarticulation for articulatory speech synthesis," *PLoS one*, vol. 8, no. 4, p. e60603, 2013.
- [13] P. K. Krug, S. Stone, and P. Birkholz, "Intelligibility and naturalness of articulatory synthesis with vocaltractlab compared to established speech synthesis technologies," *Proc. SSW*, vol. 11, pp. 102–107, 2021.
- [14] P. Wu, S. Watanabe, L. Goldstein, A. W. Black, and G. K. Anumanchipalli, "Deep speech synthesis from articulatory representations," *arXiv preprint arXiv:2209.06337*, 2022.
- [15] M. Kim, Z. Piao, J. Lee, and H.-G. Kang, "Style modeling for multi-speaker articulation-to-speech," in *ICASSP 2023-2023 IEEE International Conference on Acoustics, Speech and Signal Processing (ICASSP)*. IEEE, 2023, pp. 1–5.
- [16] Y. Gao, P. Birkholz, and Y. Li, "Articulatory copy synthesis based on the speech synthesizer vocaltractlab and convolutional recurrent neural networks," *IEEE/ACM Transactions on Audio, Speech, and Language Processing*, 2024.
- [17] P. Wu, L.-W. Chen, C. J. Cho, S. Watanabe, L. Goldstein, A. W. Black, and G. K. Anumanchipalli, "Speaker-independent acoustic-to-articulatory speech inversion," in *ICASSP 2023-2023 IEEE International Conference on Acoustics, Speech and Signal Processing (ICASSP)*. IEEE, 2023, pp. 1–5.
- [18] H.-S. Choi, J. Lee, W. Kim, J. Lee, H. Heo, and K. Lee, "Neural analysis and synthesis: Reconstructing speech from self-supervised representations," *Advances in Neural Information Processing Systems*, vol. 34, pp. 16 251–16 265, 2021.
- [19] H.-S. Choi, J. Yang, J. Lee, and H. Kim, "Nansy++: Unified voice synthesis with neural analysis and synthesis," *arXiv preprint arXiv:2211.09407*, 2022.
- [20] N. Zeghidour, A. Luebs, A. Omran, J. Skoglund, and M. Tagliasacchi, "Soundstream: An end-to-end neural audio codec," *IEEE/ACM Transactions on Audio, Speech, and Language Processing*, vol. 30, pp. 495–507, 2021.
- [21] A. Défossez, J. Copet, G. Synnaeve, and Y. Adi, "High fidelity neural audio compression," *arXiv preprint arXiv:2210.13438*, 2022.
- [22] Z. Ju, Y. Wang, K. Shen, X. Tan, D. Xin, D. Yang, Y. Liu, Y. Leng, K. Song, S. Tang *et al.*, "Naturalspeech 3: Zero-shot speech synthesis with factorized codec and diffusion models," *arXiv preprint arXiv:2403.03100*, 2024.
- [23] T. Rebernik, J. Jacobi, R. Jonkers, A. Noiray, and M. Wieling, "A review of data collection practices using electromagnetic articulography," *Laboratory Phonology*, vol. 12, no. 1, p. 6, 2021.
- [24] P. K. Ghosh and S. Narayanan, "A generalized smoothness criterion for acoustic-to-articulatory inversion," *The Journal of the Acoustical Society of America*, vol. 128, no. 4, pp. 2162–2172, 2010.
- [25] P. K. Ghosh and S. S. Narayanan, "A subject-independent acoustic-to-articulatory inversion," in *2011 IEEE International Conference on Acoustics, Speech and Signal Processing (ICASSP)*. IEEE, 2011, pp. 4624–4627.
- [26] P. Liu, Q. Yu, Z. Wu, S. Kang, H. Meng, and L. Cai, "A deep recurrent approach for acoustic-to-articulatory inversion," in *2015 IEEE International Conference on Acoustics, Speech and Signal Processing (ICASSP)*. IEEE, 2015, pp. 4450–4454.
- [27] A. A. Attia, Y. M. Siriwardena, and C. Espy-Wilson, "Improving speech inversion through self-supervised embeddings and enhanced tract variables," *arXiv preprint arXiv:2309.09220*, 2023.
- [28] Y. M. Siriwardena and C. Espy-Wilson, "The secret source: Incorporating source features to improve acoustic-to-articulatory speech inversion," in *ICASSP 2023-2023 IEEE International Conference on Acoustics, Speech and Signal Processing (ICASSP)*. IEEE, 2023, pp. 1–5.
- [29] M. G. Rahim, C. C. Goodyear, W. B. Kleijn, J. Schroeter, and M. M. Sondhi, "On the use of neural networks in articulatory speech synthesis," *The Journal of the Acoustical Society of America*, vol. 93, no. 2, pp. 1109–1121, 1993.
- [30] H. Dudley, R. R. Riesz, and S. S. Watkins, "A synthetic speaker," *Journal of the Franklin Institute*, vol. 227, no. 6, pp. 739–764, 1939.
- [31] H. Dudley, "Remaking speech," *The Journal of the Acoustical Society of America*, vol. 11, no. 2, pp. 169–177, 1939.
- [32] H. K. Dunn, "The calculation of vowel resonances, and an electrical vocal tract," *The Journal of the Acoustical Society of America*, vol. 22, no. 6, pp. 740–753, 1950.
- [33] K. N. Stevens, S. Kasowski, and C. G. M. Fant, "An electrical analog of the vocal tract," *The Journal of the Acoustical Society of America*, vol. 25, no. 4, pp. 734–742, 1953.
- [34] G. Rosen, "Dynamic analog speech synthesizer," *The Journal of the Acoustical Society of America*, vol. 30, no. 3, pp. 201–209, 1958.
- [35] P. Mermelstein, "Articulatory model for the study of speech production," *The Journal of the Acoustical Society of America*, vol. 53, no. 4, pp. 1070–1082, 1973.
- [36] P. Rubin, T. Baer, and P. Mermelstein, "An articulatory synthesizer for perceptual research," *The Journal of the Acoustical Society of America*, vol. 70, no. 2, pp. 321–328, 1981.
- [37] S. Maeda, "A digital simulation method of the vocal-tract system," *Speech communication*, vol. 1, no. 3-4, pp. 199–229, 1982.
- [38] C. Scully, "Articulatory synthesis," in *Speech production and speech modelling*. Springer, 1990, pp. 151–186.
- [39] S. Aryal and R. Gutierrez-Osuna, "Accent conversion through cross-speaker articulatory synthesis," in *2014 IEEE International Conference on Acoustics, Speech and Signal Processing (ICASSP)*. IEEE, 2014, pp. 7694–7698.
- [40] P. Birkholz, L. Martin, Y. Xu, S. Scherbaum, and C. Neuschaefer-Rube, "Manipulation of the prosodic features of vocal tract length, nasality and articulatory precision using articulatory synthesis," *Computer Speech & Language*, vol. 41, pp. 116–127, 2017.
- [41] S. Aryal and R. Gutierrez-Osuna, "Data driven articulatory synthesis with deep neural networks," *Computer Speech & Language*, vol. 36, pp. 260–273, 2016.
- [42] A. Van Den Oord, O. Vinyals *et al.*, "Neural discrete representation learning," *Advances in neural information processing systems*, vol. 30, 2017.
- [43] X. Zhang, D. Zhang, S. Li, Y. Zhou, and X. Qiu, "Speechtokenizer: Unified speech tokenizer for speech large language models," *arXiv preprint arXiv:2308.16692*, 2023.
- [44] A. Polyak, Y. Adi, J. Copet, E. Kharitonov, K. Lakhotia, W.-N. Hsu, A. Mohamed, and E. Dupoux, "Speech resynthesis from discrete disentangled self-supervised representations," *arXiv preprint arXiv:2104.00355*, 2021.
- [45] S.-H. Lee, S.-B. Kim, J.-H. Lee, E. Song, M.-J. Hwang, and S.-W. Lee, "Hierspeech: Bridging the gap between text and speech by hierarchical variational inference using self-supervised representations for speech synthesis," *Advances in Neural Information Processing Systems*, vol. 35, pp. 16 624–16 636, 2022.
- [46] S.-H. Lee, H.-Y. Choi, S.-B. Kim, and S.-W. Lee, "Hierspeech++: Bridging the gap between semantic and acoustic representation of speech by hierarchical variational inference for zero-shot speech synthesis," *arXiv preprint arXiv:2311.12454*, 2023.

- [47] H. Guo, C. Liu, C. T. Ishi, and H. Ishiguro, "Quickvc: Any-to-many voice conversion using inverse short-time fourier transform for faster conversion," *arXiv preprint arXiv:2302.08296*, 2023.
- [48] S. Chen, Y. Wu, C. Wang, S. Liu, Z. Chen, P. Wang, G. Liu, J. Li, J. Wu, X. Yu *et al.*, "Why does self-supervised learning for speech recognition benefit speaker recognition?" *arXiv preprint arXiv:2204.12765*, 2022.
- [49] A. Pasad, B. Shi, and K. Livescu, "Comparative layer-wise analysis of self-supervised speech models," in *ICASSP 2023-2023 IEEE International Conference on Acoustics, Speech and Signal Processing (ICASSP)*. IEEE, 2023, pp. 1–5.
- [50] K. Richmond, P. Hoole, and S. King, "Announcing the electromagnetic articulography (day 1) subset of the mngu0 articulatory corpus," in *Twelfth Annual Conference of the International Speech Communication Association*, 2011.
- [51] S. Chen, C. Wang, Z. Chen, Y. Wu, S. Liu, Z. Chen, J. Li, N. Kanda, T. Yoshioka, X. Xiao *et al.*, "Wavlm: Large-scale self-supervised pre-training for full stack speech processing," *IEEE Journal of Selected Topics in Signal Processing*, vol. 16, no. 6, pp. 1505–1518, 2022.
- [52] Y. Yang, Y. Kartynnik, Y. Li, J. Tang, X. Li, G. Sung, and M. Grundmann, "Streamvc: Real-time low-latency voice conversion," *arXiv preprint arXiv:2401.03078*, 2024.
- [53] J. W. Kim, J. Salamon, P. Li, and J. P. Bello, "Crep: A convolutional representation for pitch estimation," in *2018 IEEE International Conference on Acoustics, Speech and Signal Processing (ICASSP)*. IEEE, 2018, pp. 161–165.
- [54] R. Netzorg, B. Yu, A. Guzman, P. Wu, L. McNulty, and G. K. Anumanchipalli, "Towards an interpretable representation of speaker identity via perceptual voice qualities," in *ICASSP 2024-2024 IEEE International Conference on Acoustics, Speech and Signal Processing (ICASSP)*. IEEE, 2024, pp. 12391–12395.
- [55] Z. Fan, M. Li, S. Zhou, and B. Xu, "Exploring wav2vec 2.0 on speaker verification and language identification," *arXiv preprint arXiv:2012.06185*, 2020.
- [56] J. Kong, J. Kim, and J. Bae, "Hifi-gan: Generative adversarial networks for efficient and high fidelity speech synthesis," *Advances in neural information processing systems*, vol. 33, pp. 17022–17033, 2020.
- [57] E. Perez, F. Strub, H. De Vries, V. Dumoulin, and A. Courville, "Film: Visual reasoning with a general conditioning layer," in *Proceedings of the AAAI conference on artificial intelligence*, vol. 32, no. 1, 2018.
- [58] Y. Koizumi, H. Zen, S. Karita, Y. Ding, K. Yatabe, N. Morioka, M. Bacchiani, Y. Zhang, W. Han, and A. Bapna, "Libritts-r: A restored multi-speaker text-to-speech corpus," *arXiv preprint arXiv:2305.18802*, 2023.
- [59] H. Zen, V. Dang, R. Clark, Y. Zhang, R. J. Weiss, Y. Jia, Z. Chen, and Y. Wu, "Libritts: A corpus derived from librispeech for text-to-speech," *arXiv preprint arXiv:1904.02882*, 2019.
- [60] C. Veaux *et al.*, "Cstr vctk corpus: English multi-speaker corpus for cstr voice cloning toolkit," *CSTR*, 2017.
- [61] R. S. McGowan, "Recovering articulatory movement from formant frequency trajectories using task dynamics and a genetic algorithm: Preliminary model tests," *Speech Communication*, vol. 14, no. 1, pp. 19–48, 1994.
- [62] A. Wrench, "Mocha: multichannel articulatory database," <http://www.cstr.ed.ac.uk/research/project/artic/mocha.html>, 1999.
- [63] M. Tiede, C. Y. Espy-Wilson, D. Goldenberg, V. Mitra, H. Nam, and G. Sivaraman, "Quantifying kinematic aspects of reduction in a contrasting rate production task," *The Journal of the Acoustical Society of America*, vol. 141, no. 5, pp. 3580–3580, 2017.
- [64] T. Saeki, D. Xin, W. Nakata, T. Koriyama, S. Takamichi, and H. Saruwatari, "Utmos: Utokyo-sarulab system for voicemos challenge 2022," *arXiv preprint arXiv:2204.02152*, 2022.
- [65] V. Pratap, Q. Xu, A. Sriram, G. Synnaeve, and R. Collobert, "Mls: A large-scale multilingual dataset for speech research," *arXiv preprint arXiv:2012.03411*, 2020.
- [66] K. Park, "Kss dataset: Korean single speaker speech dataset," *Kss dataset: Korean single speaker speech dataset*, 2018.
- [67] S. Takamichi, K. Mitsui, Y. Saito, T. Koriyama, N. Tanji, and H. Saruwatari, "Jvs corpus: free japanese multi-speaker voice corpus," *arXiv preprint arXiv:1908.06248*, 2019.
- [68] Y. Shi, H. Bu, X. Xu, S. Zhang, and M. Li, "Aishell-3: A multi-speaker mandarin tts corpus and the baselines," *arXiv preprint arXiv:2010.11567*, 2020.
- [69] D. Snyder, D. Garcia-Romero, G. Sell, D. Povey, and S. Khudanpur, "X-vectors: Robust dnn embeddings for speaker recognition," in *2018 IEEE international conference on acoustics, speech and signal processing (ICASSP)*. IEEE, 2018, pp. 5329–5333.
- [70] H. Wang, C. Liang, S. Wang, Z. Chen, B. Zhang, X. Xiang, Y. Deng, and Y. Qian, "Wespeaker: A research and production oriented speaker embedding learning toolkit," in *ICASSP 2023-2023 IEEE International Conference on Acoustics, Speech and Signal Processing (ICASSP)*. IEEE, 2023, pp. 1–5.
- [71] A. Nagrani, J. S. Chung, and A. Zisserman, "Voxceleb: a large-scale speaker identification dataset," *arXiv preprint arXiv:1706.08612*, 2017.
- [72] J. S. Chung, A. Nagrani, and A. Zisserman, "Voxceleb2: Deep speaker recognition," *arXiv preprint arXiv:1806.05622*, 2018.
- [73] A. Nagrani, J. S. Chung, W. Xie, and A. Zisserman, "Voxceleb: Large-scale speaker verification in the wild," *Computer Speech & Language*, vol. 60, p. 101027, 2020.
- [74] E. Casanova, J. Weber, C. D. Shulby, A. C. Junior, E. Gölge, and M. A. Ponti, "Yourtts: Towards zero-shot multi-speaker tts and zero-shot voice conversion for everyone," in *International Conference on Machine Learning*. PMLR, 2022, pp. 2709–2720.
- [75] B. H. Story, "A parametric model of the vocal tract area function for vowel and consonant simulation," *The Journal of the Acoustical Society of America*, vol. 117, no. 5, pp. 3231–3254, 2005.
- [76] J.-F. Patri, J. Diard, and P. Perrier, "Optimal speech motor control and token-to-token variability: a bayesian modeling approach," *Biological cybernetics*, vol. 109, pp. 611–626, 2015.
- [77] T. Rakotomalala, P. Perrier, and P. Baraduc, "Trajectories predicted by optimal speech motor control using lstm networks," in *Interspeech 2022-23rd Annual Conference of the International Speech Communication Association*. ISCA; ISCA, 2022, pp. 630–634.
- [78] P. Badin, Y. Tarabalka, F. Elisei, and G. Bailly, "Can you 'read' tongue movements? evaluation of the contribution of tongue display to speech understanding," *Speech Communication*, vol. 52, no. 6, pp. 493–503, 2010.
- [79] A. Suemitsu, J. Dang, T. Ito, and M. Tiede, "A real-time articulatory visual feedback approach with target presentation for second language pronunciation learning," *The Journal of the Acoustical Society of America*, vol. 138, no. 4, pp. EL382–EL387, 2015.
- [80] B. Bernhardt, B. Gick, P. Bacsfalvi, and J. Ashdown, "Speech habilitation of hard of hearing adolescents using electropalatography and ultrasound as evaluated by trained listeners," *Clinical Linguistics & Phonetics*, vol. 17, no. 3, pp. 199–216, 2003.
- [81] J. Lian, A. W. Black, L. Goldstein, and G. K. Anumanchipalli, "Deep neural convolutive matrix factorization for articulatory representation decomposition," *arXiv preprint arXiv:2204.00465*, 2022.
- [82] J. Lian, A. W. Black, Y. Lu, L. Goldstein, S. Watanabe, and G. K. Anumanchipalli, "Articulatory representation learning via joint factor analysis and neural matrix factorization," in *ICASSP 2023-2023 IEEE International Conference on Acoustics, Speech and Signal Processing (ICASSP)*. IEEE, 2023, pp. 1–5.
- [83] C. J. Cho, A. Mohamed, S.-W. Li, A. W. Black, and G. K. Anumanchipalli, "Sd-hubert: Sentence-level self-distillation induces syllabic organization in hubert," in *ICASSP 2024-2024 IEEE International Conference on Acoustics, Speech and Signal Processing (ICASSP)*. IEEE, 2024, pp. 12076–12080.
- [84] A. Ji, J. J. Berry, and M. T. Johnson, "The electromagnetic articulography mandarin accented english (ema-mae) corpus of acoustic and 3d articulatory kinematic data," in *2014 IEEE International Conference on Acoustics, Speech and Signal Processing (ICASSP)*. IEEE, 2014, pp. 7719–7723.
- [85] K. He, X. Zhang, S. Ren, and J. Sun, "Deep residual learning for image recognition," in *Proceedings of the IEEE conference on computer vision and pattern recognition*, 2016, pp. 770–778.